Rabow, L., Stubbe, J., Kozarich, J. W., & Gerlt, J. A. (1986) *J. Am. Chem. Soc. 108*, 7130–7131.

Rhaese, H.-J., & Freese, E. (1968) *Biochim. Biophys. Acta 155*, 476–490.

Saenger, W. (1983) in *Principles of Nucleic Acid Structure* (Cantor, C. R., Ed.) p 221, Springer-Verlag, New York.

Sinha, N. D., Biernat, J., McManus, J., & Koster, H. (1984) *Nucleic Acids Res. 12*, 4539–4557.

Sugiyama, H., Xu, C., Murugesan, N., & Hecht, S. M. (1985) *J. Am. Chem. Soc. 107*, 4104–4105.

Wu, J. C., Kozarich, J. W., & Stubbe, J. (1983) *J. Biol. Chem. 258*, 4694–4697.

Wu, J. C., Kozarich, J. W., & Stubbe, J. (1985a) *Biochemistry 24*, 7562–7568.

Wu, J. C., Stubbe, J., & Kozarich, J. W. (1985b) *Biochemistry 24*, 7569–7573.

NMR Studies of the Interaction of the Antibiotic Nogalamycin with the Hexadeoxyribonucleotide Duplex d(5'-GCATGC)2[†]

Mark S. Searle,[‡] Jon G. Hall,[‡] William A. Denny,[§] and Laurence P. G. Wakelin*[,‡]

Molecular Pharmacology Group and NMR Facility, Peter MacCallum Cancer Institute, Melbourne, Victoria 3000, Australia, and Cancer Research Laboratory, School of Medicine, University of Auckland, Auckland, New Zealand

Received August 27, 1987; Revised Manuscript Received February 2, 1988

ABSTRACT: [1]H resonance assignments in the NMR spectra of the self-complementary hexadeoxyribonucleoside pentaphosphate d(5'-GCATGC)2 and its complex with the antibiotic nogalamycin, together with interproton distance constraints obtained from two-dimensional nuclear Overhauser effect (NOE) spectra, have enabled us to characterize the three-dimensional structure of these species in solution. In the complex described, two drug molecules are bound per duplex, in each of two equivalent binding sites, with full retention of the dyad symmetry. Twenty-eight NOE distance constraints between antibiotic and nucleotide protons define the position and orientation of the bound drug molecule. Nogalamycin intercalates at the 5'-CA and 5'-TG steps with the major axis of the anthracycline chromophore aligned approximately at right angles to the major axes of the base pairs. The nogalose sugar occupies the minor groove of the helix and makes many contacts with the deoxyribose moieties of three nucleotides along one strand of the duplex in the 5'-TGC segment. The charged dimethylamino group and hydroxyl functions of the bicyclic sugar lie in the major groove juxtaposed to the guanine base, the bridging atoms of the bicyclic sugar making contacts with the methyl group of the thymine. Thus the antibiotic is not symmetrically disposed in the intercalation site but is in close contact in both grooves with atoms comprising the 5'-TGC strand. The intercalation cavity is wedge-shaped, the major axes of the base pairs forming the site being tilted with respect to one another. All base-pair hydrogen-bonding interactions are maintained in the complex, and there is no evidence for Hoogsteen pairing. The free duplex adopts a regular right-handed B-type conformation in which all glycosidic bond angles are anti and all sugar puckers lie in the C2'-endo range. In the complex the glycosidic bond angles and the sugar puckers deviate little from those observed for the duplex alone. The presence of two bound nogalamycin molecules substantially slows the "breathing" motions of the base pairs forming the intercalation cavity, and the observation of two downfield-shifted resonances in the ^{31}P NMR spectrum of the complex suggests a pronounced local helix unwinding at the drug binding site. The footprinting data of Fox and Waring [Fox, K. R., & Waring, M. J. (1986) *Biochemistry 25*, 4349–4356] imply that the highest affinity binding sites of nogalamycin have the sequence 5'-GCA (or 5'-TGC). Our findings show that the major determinants of specificity appear to be hydrogen-bonding interactions between the O6 and N7 atoms of the guanine in the intercalation site and the two hydroxyl groups of the bicyclic sugar of the antibiotic, coupled with hydrogen-bonding/electrostatic interaction between the protonated dimethylamino group and the O6 carbonyl of the terminal guanine.

Nogalamycin (Figure 1) is an anthracycline antibiotic active against Gram-positive bacteria and experimental tumours (Bhuyan & Dietz, 1965; Bhuyan & Reusser, 1970; Li et al., 1979). It is a selective inhibitor of DNA-directed RNA synthesis in prokaryotic and eukaryotic organisms (Fok &

Waring, 1972; Li et al., 1979; Ennis, 1981), and its interaction with DNA has been well studied. It has been shown to be an intercalating agent by its capacity to both remove and reverse the supercoiling of circular DNA (Gale et al., 1981) and to increase the viscosity and contour length of linear DNA (Kersten et al., 1966; Das et al., 1974; Sinha et al., 1977). As is typical of intercalators, it decreases DNA buoyant density and sedimentation coefficient (Kersten et al., 1966) and stabilizes DNA toward thermal denaturation (Kersten et al., 1966; Das et al., 1974; Sinha et al., 1977). The intrinsic affinity of nogalamycin for eukaryotic DNAs is of the order
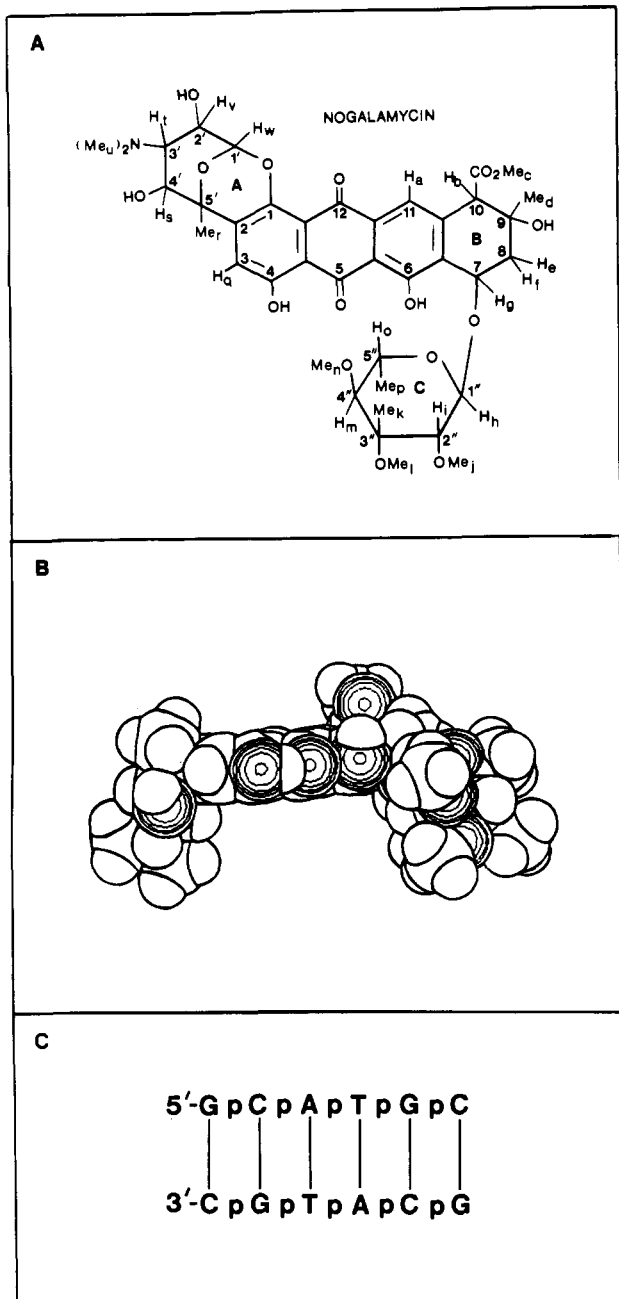
FIGURE 1: (A) Chemical structure, numbering scheme, and labeling of protons of nogalamycin. (B) Space-filling representation of nogalamycin illustrating the bulky sugar moieties at either end of the chromophore. (C) Schematic representation of duplex under study; nucleotide residues are numbered sequentially from the 5' end of the hexamer, viz., d(1G2C3A4T5G6C).

the sequence 5'-GCA and its equivalent 5'-TGC. Not one of the sites with these sequences is left unprotected by nogalamycin in the three DNA fragments Fox and Waring (1986) describe. Thus it would seem that the most highly favored binding site for the antibiotic in natural DNA is to be found at the trinucleotide sequence 5'-GCA (or 5'-TGC). The crystal and molecular structure of nogalamycin has been determined by Arora (1983), which led him to propose a model for its DNA complex. He suggests that the anthracycline ring is intercalated with its major axis at right angles to the major axis of the base pairs so that the bicyclo amino group and the nogalose sugar moiety of nogalamycin are located in the wide and narrow grooves of the helix, respectively (Arora, 1983). Computer graphics and nonbonded energy calculations have confirmed the plausibility of this model and revealed that the alternative arrangement, with the antibiotic rotated through 180°, is also energetically feasible (Collier et al., 1984).

Two experimental approaches are available for establishing the three-dimensional structure of DNA/drug complexes at, or near, atomic resolution: namely, X-ray crystallography and NMR spectroscopy. The latter technique has the advantages of providing information about the system in solution and also yields insights into dynamic processes. We report here NMR studies of the structure of a nogalamycin/hexadeoxyribonucleotide complex which, with regard to the disposition of the nogalamycin sugars at least, reveal intercalative binding in general accord with Arora's model. We chose the self-complementary duplex d(GCATGC)$_2$ for study since this contains two symmetrically equivalent GCA and TGC nogalamycin binding sites [see Fox and Waring (1986) and above], and thus the 2:1 nogalamycin/duplex complex retains the twofold symmetry of the free DNA. This is experimentally advantageous since we observe NMR signals from only one strand of DNA and one drug molecule. The starting point for any characterization of conformation and dynamics in small DNA duplexes, or their drug complexes, requires sequence-specific assignment of resonances in complicated ^{1}H NMR spectra. Strategies for making these assignments are now well established (Hare et al., 1983; Scheek et al., 1983; Clore & Gronenborn, 1985; Chazin et al., 1986). The positions and orientations of bound drug molecules are revealed by intermolecular NOESY[1] contacts and by perturbations to the ^{31}P and ^{1}H chemical shifts of the phosphate groups and nucleotide proton resonances. ^{1}H and ^{31}P resonance assignments for this hexanucleotide have been reported previously (Frey et al., 1985).

MATERIALS AND METHODS

The hexadeoxyribonucleoside pentaphosphate d(5'-GCATGC)$_2$ was prepared by a modified version of the phosphotriester method as described by Denny et al. (1982) and also by Frey et al. (1985). Nogalamycin was a gift from Dr. P. F. Wiley of the Upjohn Company, Kalamazoo, MI, and was used without further purification. The hexanucleotide was dissolved in 650 µL of buffered D$_2$O solution containing 40 mM NaCl and 10 mM NaD$_2$PO$_4$ at pD 6.90. The material was lyophilized twice from 99.96% D$_2$O and the hexanucleotide finally dissolved in 650 µL of 99.996% D$_2$O (Aldrich Chemical Co.). The concentration of the duplex was 5.0 mM for studies

5×10^5 M^{-1} with maximum measured levels of binding in the region of 0.3–0.4 drug molecule per base pair (Das et al., 1974; Sinha et al., 1977); by contrast, binding to RNA is barely detectable (Plumbridge & Brown, 1979). Early studies aimed at determining potential nucleotide sequence preferences in the binding of nogalamycin produced conflicting results, some authors reporting an AT selectivity (Bhuyan & Smith, 1965), some a GC selectivity (Kersten et al., 1966), and yet others finding no sequence preferences (Chowdhury et al., 1978). More recently, Fox and Waring (1986), using footprinting methods, report that nogalamycin binds preferentially, but not exclusively, to the dinucleotide steps TpG (CpA) and GpT (ApC) located in regions of alternating purine–pyrimidine sequences. However, careful scrutiny of their data reveals that the large majority of endonuclease-protected regions occur at

---

Table I: ^{1}H NMR Chemical Shifts[a] of d(GCATGC)$_2$ and the (Nogalamycin)$_2$/d(GCATGC)$_2$ Complex

nucleotide	H1'	H2'	H2''	H3'	H4'	H5'/5''	H2	H5	H6	H8	N1H	N3H
						Chemical Shifts of d(GCATGC)$_2$						
1G	5.83	2.53	2.70	4.75	4.21	3.65/3.65				7.83		
2C	5.58	2.07	2.41	4.82	4.13	4.02/4.02		5.28	7.36			
3A	6.19	2.66	2.87	4.97	4.37	4.10/4.00	7.60			8.27		
4T	5.61	1.87	2.26	4.78	4.10	4.19/4.22		1.39	7.01			13.68[b]
5G	5.82	2.50	2.61	4.89	4.29	4.02/4.01				7.73	12.85[b]	
6C	6.00	2.10	2.16	4.41	3.95	3.98/3.98		5.08	7.22			
						Chemical Shifts of (Nogalamycin)$_2$/d(GCATGC)$_2$						
1G	5.87	2.56	2.67	4.84	3.81	4.22				7.95		
2C	6.09	2.54	2.26	5.04	4.36	4.13/4.28		5.46	7.48			
3A	6.42	2.49	2.94	4.99	4.56		7.95			8.43		
4T	6.13	2.66	2.60	5.06	4.29			1.18	7.16			12.93
5G	5.61	2.52	2.62	4.95	4.57	4.44/4.28				6.75	12.84	
6C	6.02	1.92	2.16	4.41	3.96	4.31		5.04	7.31			

Nogalamycin Chemical Shifts—Bound (Free)

H_a	7.03 (6.90)	H_h	5.24 (5.22)	OMe_n	3.54 (3.72)	H_t	4.29 (3.81)
H_b	4.17 (3.91)	H_i	3.08 (3.02)	H_o	3.86 (3.38)	Me_u	2.87 (2.53)
Me_c	3.87 (3.82)	OMe_j	3.67 (3.35)	Me_p	1.42 (1.24)	H_v	4.18 (4.06)
Me_d	1.54 (1.35)	Me_k	1.34 (1.01)	H_q	6.92 (6.81)	H_w	5.70 (5.47)
H_e/H_f	1.94, 2.98 (1.96, 2.63)	OMe_l	3.18 (3.00)	Me_r	1.61 (1.56)	H_A	10.72
H_g	4.73 (4.86)	H_m	3.18 (3.03)	H_s	3.89 (3.94)	H_B	11.67

[a] All chemical shifts ±0.01 ppm at 20 °C. [b] Chemical shifts recorded at 2 °C.

of the duplex alone and 3.9 mM for studies of its 1:2 nogalamycin complex. Nogalamycin was dissolved in 20 mM DCl in D$_2$O to a concentration of 100 mM. The pD was adjusted to pD 7.0 with NaOD in D$_2$O, and aliquots of 5–10 μL of the antibiotic solution were slowly added to the duplex with vigorous stirring. The stoichiometry of the nogalamycin/d-(GCATGC)$_2$ complex was monitored by ^{1}H NMR.

NMR measurements were made on a Varian VXR 400 spectrometer. Homonuclear ^{1}H double-quantum-filtered COSY and NOESY experiments were performed in the phase-sensitive mode according to the hypercomplex method (Muller & Ernst, 1979; States et al., 1982; Rance et al., 1983; Williamson, 1983; Keeler & Neuhaus, 1985). Data were collected with the carrier frequency placed at the center of the spectrum by using a spectral width of 3000 Hz with quadrature detection in both dimensions. Data were recorded as 1024 points in t_2 for each of 320–512 t_1 values. A relaxation delay of 1.4–1.6 s was incorporated into each sequence. The total data accumulation time ranged from 16 to 36 h. The data were zero-filled to 1024 points in t_1 prior to Fourier transformation. An apodization function was used to weight the data to ensure that the interferogram decayed to zero by the end of data accumulation, thus avoiding truncation of the free induction decays.

^{1}H NMR spectra of the exchangeable proton resonances were collected in 90% H$_2$O/10% D$_2$O by using the 1:1 pulse sequence (Clore et al., 1983; Hore, 1983) to give on-resonance suppression of the solvent peak. One-dimensional NOE experiments in H$_2$O were similarly performed by using the 1:1 water suppression sequence with NOE difference spectra obtained from data sets collected in the interleaved mode with an on-resonance and off-resonance selective irradiation immediately prior to acquisition. A selective preirradiation period of 300 ms was used with a 2-s relaxation delay. It is interesting to note that in the drug–DNA complex the stability of the base-pair hydrogen bonds was sufficiently great to enable ^{1}H NMR spectra to be obtained in H$_2$O by using more conventional selective saturation methods to suppress the residual solvent peak. This method led to only partial saturation of the imino proton resonances through saturation transfer, even at 20 °C. ^{31}P NMR spectra were recorded at a frequency of 160 MHz with the same 650 μL of solution used for ^{1}H studies. All spectra were obtained with ^{1}H decoupling over

a 2000-Hz sweep width. A π/4 excitation pulse was used with a 2-s relaxation delay prior to acquisition. ^{1}H chemical shifts are referenced to 3-(trimethylsilyl)propionic acid, and ^{31}P chemical shifts are referenced to the resonance from the phosphate buffer at pH 7.0.

RESULTS AND DISCUSSION

^{1}H Resonance Assignments and Structural Characterization of d(GCATGC)$_2$. Resonances in the ^{1}H NMR spectrum of d(GCATGC)$_2$ were assigned according to established methods (Reid et al., 1983; Scheek et al., 1983; Clore & Gronenborn, 1985; Chazin et al., 1986). First, DQF-COSY was used to delineate through-bond scalar coupling interactions, for example, to identify H1', H2'/2'', H3', and H4' protons within each of the six sugar ring systems. Second, NOESY data recorded at a short mixing time (60 ms) enabled residues to be assigned sequentially along the strand by identifying cross-peaks corresponding to the short interproton distances $d_i(6,8;2')$ and $d_s(6,8;2'')$. The chemical shift values of all assigned resonances are listed in Table I. From a series of NOESY spectra recorded with mixing times of 60, 90, 120, and 250 ms a quantitative comparison of NOE cross-peak intensities together with the pattern of correlations leads us to conclude that d(GCATGC)$_2$ forms a right-handed B-type structure in solution in which the sugar puckers lie in the C2'-endo region with glycosidic bond angles in the anti range (Nilges et al., 1987).

^{1}H Resonance Assignments and Structural Characterization of the (Nogalamycin)$_2$/d(GCATGC)$_2$ Complex. The ^{1}H NMR spectra of d(GCATGC)$_2$, nogalamycin, and the (nogalamycin)$_2$/d(GCATGC)$_2$ complex recorded at 20 °C are shown in Figure 2. The spectrum of the complex containing two bound drug molecules per duplex shows full retention of the dyad symmetry observed for d(GCATGC)$_2$ alone. Thus, with this stoichiometry the increase in complexity of the spectrum is kept to a minimum and only a single set of resonances is observed for each of the six nucleotides in the sequence. Similarly, only one set of bound drug resonances is observed. The aromatic region of the spectrum of the complex between 6.5 and 8.5 ppm contains two uniquely resolved singlet resonances, in addition to the four resonances expected from the nucleotide, corresponding to the drug protons H_a and H_q. The line widths of all of the singlet
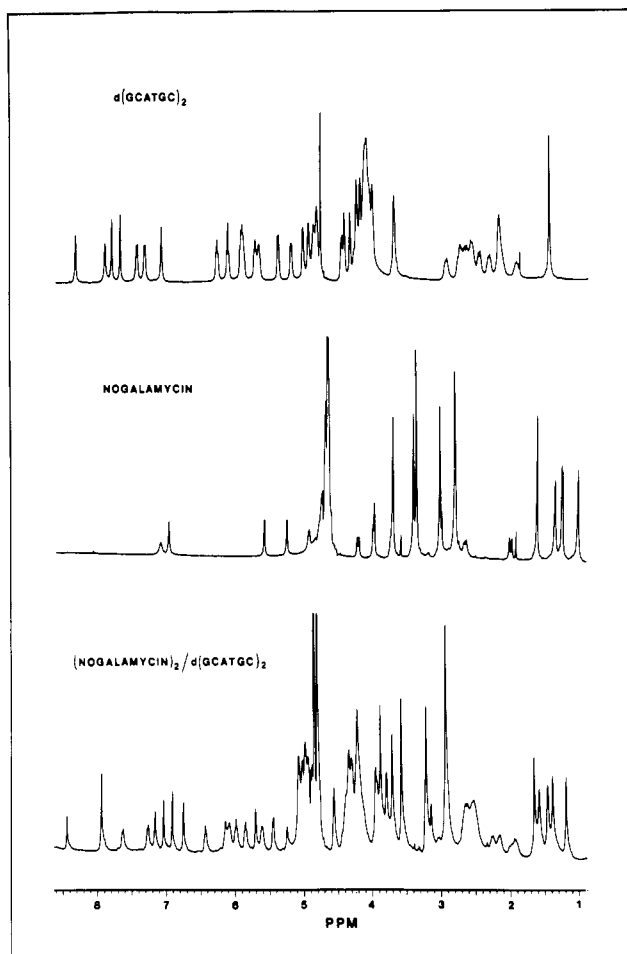
FIGURE 2: One-dimensional ^{1}H NMR spectra of d(GCATGC)$_2$, nogalamycin, and the (nogalamycin)$_2$/d(GCATGC)$_2$ complex recorded at 20 °C.
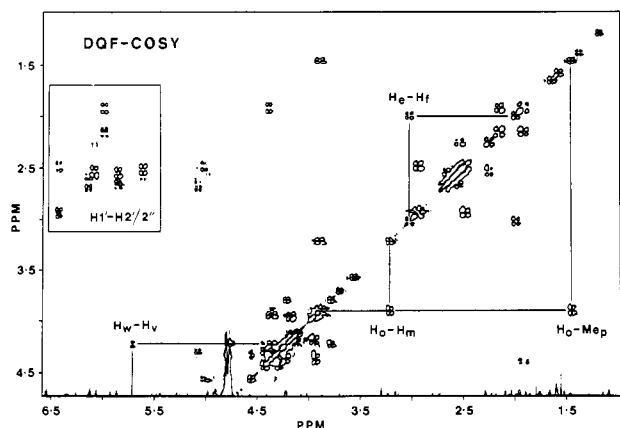

FIGURE 3: Expansion of the DQF-COSY spectrum of the (nogalamycin)$_2$/d(GCATGC)$_2$ complex. Continuous lines identify some scalar coupling interactions between protons on the bound drug molecule (see Figure 1 for labeling of drug protons). The boxed region contains the cross-peaks H1'–H2' and H1'–H2'' for the six nucleotide sugar rings.

resonances in this part of the spectrum from both the drug and nucleotide are similar (3 Hz) and are characteristic of a complexed drug molecule in slow exchange on the chemical shift time scale. The strategy we use for obtaining ^{1}H resonance assignments in the spectrum of the complex is similar to that described for the DNA alone.

d(GCATGC)$_2$ Resonance Assignments in the Complex. The spin systems of the six deoxyribose rings are partially identified in the DQF-COSY spectrum of Figure 3. The correlations
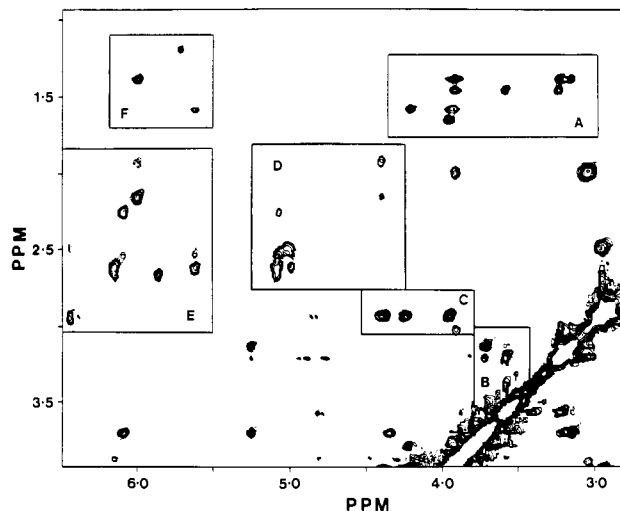

FIGURE 4: Expanded region of the NOESY spectrum of the (nogalamycin)$_2$/d(GCATGC)$_2$ complex, recorded at 20 °C with a mixing time of 100 ms. The boxed regions contain the following correlations referred to in the text: Box A reveals that Me$_k$ is close to H$_j$, OMe$_l$, and H$_o$, that Me$_p$ is close to OMe$_l$, OMe$_n$, and H$_o$, that Me$_d$ is close to H$_b$ and OMe$_c$, and that Me$_r$ is close to H$_s$. In Box B correlations are observed from OMe$_j$ to OMe$_l$ and H$_i$ and from OMe$_n$ to OMe$_l$. Box C identifies correlations between Me$_u$ and H$_s$, H$_t$, and H$_v$. Boxes D and E contain intranucleotide cross-peaks between H2'/H2'' and H3' and between H1' and H2'/H2'', respectively. In Box F several correlations are observed between drug and DNA protons, namely, H$_w$–4TCH$_3$, 6CH1'–Me$_k$, and 5GH1'–Me$_d$.

between the H1' and H2'/H2'' protons are highlighted. Further correlations between the H2'/H2'' and H3' protons and between the H3' and H4' protons are also observed for a number, but not all, of the sugar moieties. Assignments were complemented by NOESY data obtained at a short mixing time (100 ms) to observe selectively short-range intraresidue NOEs. Some of these correlations are highlighted in the portion of the NOESY spectrum illustrated in Figure 4. Thus a combination of NOESY and DQF-COSY has enabled all but a few H5'/H5'' sugar protons to be assigned. Correlation between H5 and H6 within each of the two cytosine bases is also readily apparent in the DQF-COSY spectrum, while the thymine 5-CH$_3$ to H6 resonances are correlated by an intense cross-peak in the NOESY spectrum. Base protons are assigned specifically in a sequential manner from the pattern of short interproton distances observed in the 100-ms NOESY spectrum. In the right-handed B-type conformation the H6 or H8 proton of a base is close ($\simeq$2.2 Å) to its own deoxyribose H2' and the H2'' of the sequential nucleotide in the 5' direction along the sequence. The H2' is distinguished from that of the H2'' within each of the six sugar rings by the relative intensity of NOESY cross-peaks from H1'. The H1' to H2'' distance is never larger than that from H1' to H2' in any of the possible ring pucker conformations and in general is much shorter when the sugar conformation lies in the C2'-endo region. On this basis we are able to distinguish the H2' from H2'' for each sugar moiety.

The sequential connectivity map in which the short distances $d_i(6,8;2')$ and $d_s(6,8;2'')$ are manifested in the NOESY spectrum are illustrated in Figure 5. The pattern of correlations is similar for both the complex and d(GCATGC)$_2$ alone, the major difference between them being pertubations in the connections that involve the 5GH8. At this point the intensity of both the intranucleotide and sequential connections are particularly weak. For the remainder of the nucleotide sequence the pattern of sequential connectivities is analogous to that expected for a B-type helix and the major pertubation
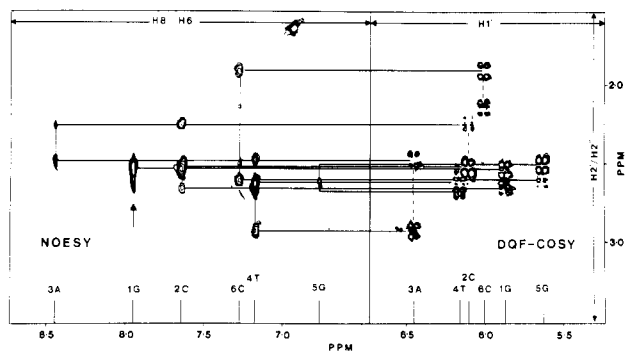
FIGURE 5: Combined DQF-COSY/NOESY connectivity diagram for obtaining sequential resonance assignments in the (nogalamycin)$_2$/d(GCATGC)$_2$ complex. The portion of the NOESY spectrum illustrated (100-ms mixing time) contains cross-peaks corresponding to the short intranucleotide and sequential nucleotide interproton distances $d_i(6,8;2')$ and $d_s(6,8;2'')$. The right-hand side of the figure contains the H1'–H2' and H1'–H2'' correlations from the DQF-COSY spectrum of the complex for each of the six deoxyribose rings. The two cross-peaks from each sugar ring are connected by broken vertical lines. Starting from the 1GH8, a NOESY cross-peak is observed corresponding to $d_i(8;2')$. The DQF-COSY connects the H2' to H2'' of this residue via a mutual coupling to the H1'. The H2'' now gives a NOESY cross-peak corresponding to the sequential connection to the 2CH6 on the 5' side of the chain. This process can be repeated along the full length of the sequence except where perturbations occur involving the 5GH8.

at the 5G position is the first indication that nogalamycin may be bound near this site. This notion is supported further by the fact that the resonances from both the 5GH8 and 4TCH$_3$ of the preceding nucleotide are shifted upfield by 0.98 and 0.21 ppm, respectively. Chemical shift values of the complexed duplex are recorded in Table I. The right-handedness of the helix is confirmed by the observation of a strong NOESY cross-peak between the 3AH8 and 4TCH$_3$ group in the A·T core of the complex, as observed in d(GCATGC)$_2$ alone. The pattern of intranucleotide NOESY cross-peak intensities leads us to propose the following distance relationship: $d_i(6,8;2') > d_i(6,8;1') > d_i(6,8;3')$, from which we conclude that the sugar pucker and glycosidic bond angles lie in the C2'-endo and anti ranges for all six nucleotides.

Nogalamycin Resonance Assignments in the Complex. The ^{1}H NMR spectra of free nogalamycin in both CDCl$_3$ and D$_2$O have been fully assigned by DQF-COSY and NOESY experiments (unpublished data), the assignments in D$_2$O providing the basis for drug resonance assignments in the complex. Five methyl resonances are apparent in the 1.0–1.5 ppm region of the spectrum of the complex at 20 °C, four of which originate from the bound drug molecule, the remaining resonance coming from the thymine base (4TCH$_3$). One of the drug methyl resonances, at 1.42 ppm, can be resolved into a doublet ($^3J = 5$ Hz) and can be unambiguously assigned to Me$_p$. Me$_p$ is coupled to H$_o$, which in turn is coupled to H$_m$. These correlations are observed in the portion of the DQF-COSY spectrum of the complex illustrated in Figure 3. Nogalamycin also gives rise to four methoxy resonances (OMe$_c$, OMe$_j$, OMe$_l$, and OMe$_n$) and an *N,N*-dimethyl resonance (Me$_u$), all of which are readily identified between 2.8 and 3.9 ppm. The Me$_u$ resonance stands out at 2.87 ppm, having twice the intensity of the methoxy resonances. The assignment of other proton resonances from the bound nogalamycin molecule is necessarily based upon NOESY data in the absence of further information from scalar coupling interactions.

The Me$_u$ resonance provides a convenient starting point for assigning resonances from protons in the bicyclic ring system. Three very intense NOESY cross-peaks involving Me$_u$ are observed at 3.89, 4.18, and 4.29 ppm which we expect to

originate from H$_s$, H$_t$, and H$_v$ since the latter are close in space to the dimethylamine group. We cannot assign these resonances specifically at this stage. The resonance from H$_w$ is expected to appear in the region of the spectrum characteristic of nucleotide H1' resonances between 5.2 and 6.5 ppm. The resonance at 5.70 ppm gives a cross-peak in the DQF-COSY spectrum to a proton at 4.18 ppm, which is in a region of the spectrum uncharacteristic of nucleotide H1'–H2'/H2'' correlations. The resonance at 4.18 ppm we conclude must be ascribed to H$_v$ which is coupled to H$_w$ at 5.70 ppm. The resonances at 4.29 and 3.89 ppm thus originate from either H$_t$ or H$_s$. The latter signal, which we ascribe to H$_s$, is assigned by a NOESY cross-peak to the methyl resonance at 1.61 ppm, which we conclude must originate from Me$_r$ since no other methyl groups (other than Me$_u$) are expected to be close to this portion of the molecule. Nogalamycin contains two aromatic protons that are expected to appear as singlets between 6.5 and 7.5 ppm. The resonance from H$_q$ is identified at 6.92 ppm on the basis of a large NOESY cross-peak to Me$_r$. The remaining aromatic singlet resonance at 7.03 ppm can thus be assigned to H$_a$ by a process of elimination, all other aromatic protons having been assigned to nucleotide resonances as described above. The resonance H$_a$ gives only a single NOESY cross-peak in the spectrum to a methoxy resonance at 3.87 ppm. This methoxy resonance in turn gives NOEs to a pair of geminal coupled protons at 1.94 and 2.98 ppm and a methyl resonance at 1.54 ppm. The geminal pair of protons we can assign unambiguously to H$_e$ and H$_f$, all other geminal pairs having been assigned to the H2'/H2'' of the six sugar rings of the DNA. From this pattern of NOESY cross-peaks it is evident that the methoxy resonance is that of OMe$_c$ and that the methyl resonance at 1.54 ppm is that of Me$_d$. These assignments are supported by additional cross-peaks between H$_e$/H$_f$ and Me$_d$ in a NOESY spectrum recorded with a mixing time of 250 ms (data not shown). The resonance from H$_b$ at 4.17 ppm is assigned by a NOESY cross-peak to Me$_d$.

The remaining unassigned methyl resonance in the 1.0–1.5 ppm region of the spectrum we attribute to Me$_k$ by a process of elimination, all others having been identified. The resonance from Me$_k$ together with those from Me$_p$, H$_o$, and H$_m$, previously identified from correlations in the DQF-COSY spectrum, provides a starting point for assignment of the remaining protons in the nogalose sugar ring. The resonance from Me$_k$ at 1.34 ppm gives a NOESY cross-peak to a single proton resonance at 3.08 ppm (not H$_m$ or H$_o$), which we conclude belongs to H$_i$. H$_i$ in turn gives NOESY cross-peaks to a methoxy resonance at 3.67 ppm and a single proton resonance at 5.24 ppm. The low-field chemical shift of this latter resonance leads us to conclude that it belongs to H$_h$. H$_h$ also gives a NOESY cross-peak to the methoxy resonance at 3.67 ppm and to a signal at 4.73 ppm. The former resonance we assign confidently to that of OMe$_j$ while the latter signal, whose intensity appears to be attenuated by irradiation of the residual water peak, we assign to H$_g$. The resonance from H$_g$ gives weak cross-peaks to H$_e$ and H$_f$ in a NOESY spectrum recorded with a longer mixing time of 250 ms (data not shown), which adds weight to its assignment. The assignment of the remaining two methoxy resonances from OMe$_l$ and OMe$_n$ we rationalize on the basis of the following pattern of NOESY cross-peaks. We conclude that the resonance at 3.18 ppm is that of OMe$_l$ giving correlation to OMe$_j$, Me$_k$, Me$_p$, and OMe$_n$ while the resonance at 3.54 ppm is that of OMe$_n$ with cross-peaks to Me$_p$ and OMe$_l$.

Site of Drug Binding and Structure of the Complex. Complete assignment of the drug resonances in the spectrum

Table II: Intermolecular NOEs in the (Nogalamycin)$_2$/d(GCATGC)$_2$ Complex

drug proton	DNA proton	drug proton	DNA proton
H$_a$	5GN1H	OMe$_l$	6CH1'
H$_b$	5GH1'	OMe$_n$	4TH1'
Me$_c$	4TH1'	H$_o$	4TH1'
Me$_d$	5GH1', 5GH4', 6CH1'	H$_q$	4TCH$_3$, 2CH5
H$_h$	3AH1'	Me$_r$	4TCH$_3$
OMe$_j$	2CH1', 3AH1'	H$_v$	5GH1', 4TH3', 5GH8
Me$_k$	6CH1', 6CH2', 6CH2''	H$_w$	4TCH$_3$, 4TH6
		H$_A$	4TN3H, 5GN1H, 3AH8
		H$_B$	3AH2, 4TN3H

of the complex together with all but a few H5'/H5'' resonances from the hexanucleotide now provides the basis for identifying drug–DNA contacts, and thus for deducing the mode of binding of nogalamycin. A list of NOE-derived DNA-to-drug interproton contacts is presented in Table II. These data were obtained from a NOESY spectrum recorded with a mixing time of 100 ms. Table II is extensive and includes nogalamycin–DNA contacts from all portions of the drug molecule. The intensity of many of the NOESY cross-peaks between drug and DNA indicates interproton distances of less than 3.0 Å. All contacts involving the nogalose sugar moiety (ring C) and anthracycline ring B are solely with DNA protons that lie in the narrow groove. These contacts involve predominantly one strand of the nucleotide, and binding encompasses the full 5'-TGC stretch. Short interproton distances (<3.0 Å) are observed between Me$_k$ and 6CH1' of the terminal nucleotide; H$_b$ and Me$_c$ are close to 5GH1'; OMe$_n$ and H$_o$ are close to 4TH1'. By contrast, the bicyclic ring system A makes contacts only in the major groove along the same 5'-TGC strand, the strongest interactions being observed between the drug protons H$_v$ and Me$_r$ and the thymine methyl group, 4TCH$_3$. Taking all together, the observed contacts between drug and duplex can only be rationalized by intercalating nogalamycin at the sequences 5'-CA and 5'-TG, with the nogalose sugar and ring B lying in the narrow groove and the bicyclic ring A positioned in the major groove. The nogalose sugar moiety essentially covers the minor groove over a span of three base pairs. This arrangement of ring systems A and C forces the major axis of the anthracycline chromophore approximately parallel to the minor axis of the base pairs in an analogous manner to that observed for daunomycin in its crystalline complex with d(CGTACG)$_2$ (Quigley et al., 1980). Our proposed configuration of the nogalamycin–hexanucleotide complex is illustrated schematically in Figure 6.

A number of intramolecular NOEs observed for the complexed but not the free drug point to additional conformational constraints in the bound form involving rotation about the O7–C1'' and O7–C7 bonds. The observation of an NOE between the drug methyl resonances Me$_d$ and Me$_k$ requires that these groups be spaced <4 Å apart. Smaller NOEs are also observed from Me$_k$ to H$_e$ and H$_f$ which are adjacent to Me$_d$ on ring A. These NOEs place considerable constraints on the possible orientations of the rings B and C. In our preliminary model the nogalose sugar ring C and ring B are in a conformation similar to that found in the crystal structure of nogalamycin (Arora, 1983), with the torsion angle C8–C7–O7–C1'' lying between 99° and 109°. The crystal structure implies an average interproton distance between Me$_k$ and Me$_d$ of 3.6 Å and between Me$_k$ and H$_e$/H$_f$ of 5.3 Å, both distances being in accord with semiquantitative interpretation of the NOE data.

Binding of nogalamycin in general induces relatively small changes in the glycosidic bond angles and sugar ring puckers
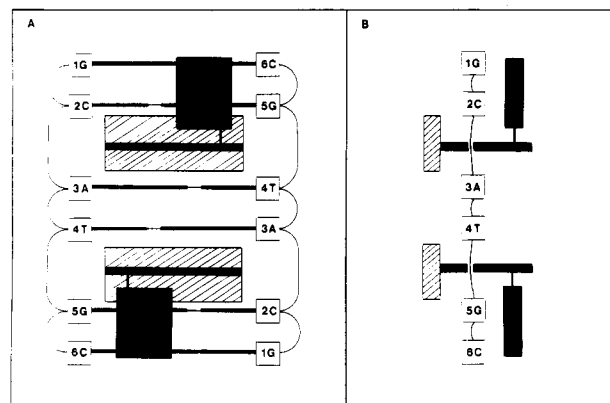

FIGURE 6: Schematic representation of the (nogalamycin)$_2$/d-(GCATGC)$_2$ complex containing two intercalated drug molecules bound in the two equivalent sites. The solid black area corresponds to the nogalose sugar ring which lies in the minor groove of the helix (view A) while the hatched area represents the bicyclo ring system which interacts with the duplex in the major groove. The chromophore threads through the helix connecting the sugar moieties in either groove (view B).

of the hexanucleotide, the duplex retaining the B-type helical conformation. NOESY cross-peaks corresponding to $d_i(6,8;1')$ for the 4T and 5G nucleotides are, however, more intense than for the other residues in the sequence, which leads us to conclude that the glycosidic bond angles are perturbed to some degree at the drug binding site. The sugar moieties of nucleotides 3A and 4T evidently deviate a little from a pure C2'-endo pucker since low-intensity COSY cross-peaks are visible for H3'–H2'' in the complex but not for d(GCATGC)$_2$ alone.

Exchangeable Proton Resonances. NMR spectra of the exchangeable protons of the free hexanucleotide and the complex, below 10.5 ppm, are illustrated in Figure 7. Dyad symmetry in both the DNA and the complex reduces the number of distinguishable imino protons to three, although under the low ionic strength conditions used here (50 mM in Na$^+$) only two of the protons exchange slowly enough to be observed in the spectrum of the free hexanucleotide. Short interproton distances within the B-type helical structure enable these imino protons to be assigned by 1D NOE experiments. Irradiating the resonance at 13.68 ppm for 300 ms results in two NOEs, one to the exchangeable proton resonance at 12.85 ppm and a second to the previously assigned 3AH2 resonance at 7.60 ppm. The large interstrand NOE to the 3AH2 resonance assigns the peak at 13.68 ppm to the thymidine N3H of the same A·T base pair. The sequential NOE to the resonance at 12.85 ppm assigns this signal to the guanine N1H of the nonterminal base pair. The NOE difference spectrum in Figure 8 illustrates the proximity of the 4TN3H, 5GN1H, and 3AH2 protons on irradiation of 3AH2 for 300 ms.

The addition of 2 mol equiv of nogalamycin to d-(GCATGC)$_2$ substantially stabilizes the duplex toward thermal denaturation, the midpoint of the helix-to-coil transition rising from 41 ± 1 to 67 ± 2 °C in the presence of the antibiotic (unpublished observations). In the low-field spectrum of the complex recorded in H$_2$O (Figure 7) four exchangeable proton resonances are observed below 10.5 ppm at 20 °C. At this temperature resonance H$_B$ is significantly more exchange broadened ($\Delta\nu_{1/2}$ = 25 Hz) than H$_A$, H$_C$, or H$_D$. These latter resonances are still readily observed at 55 °C, where exchange broadening remains minimal ($\Delta\nu_{1/2}$ < 10 Hz). By comparison, at temperatures above 25 °C resonances from the duplex alone are sufficiently exchange broadened ($\Delta\nu_{1/2}$ > 150 Hz) as to be unobservable (Figure 7). The two
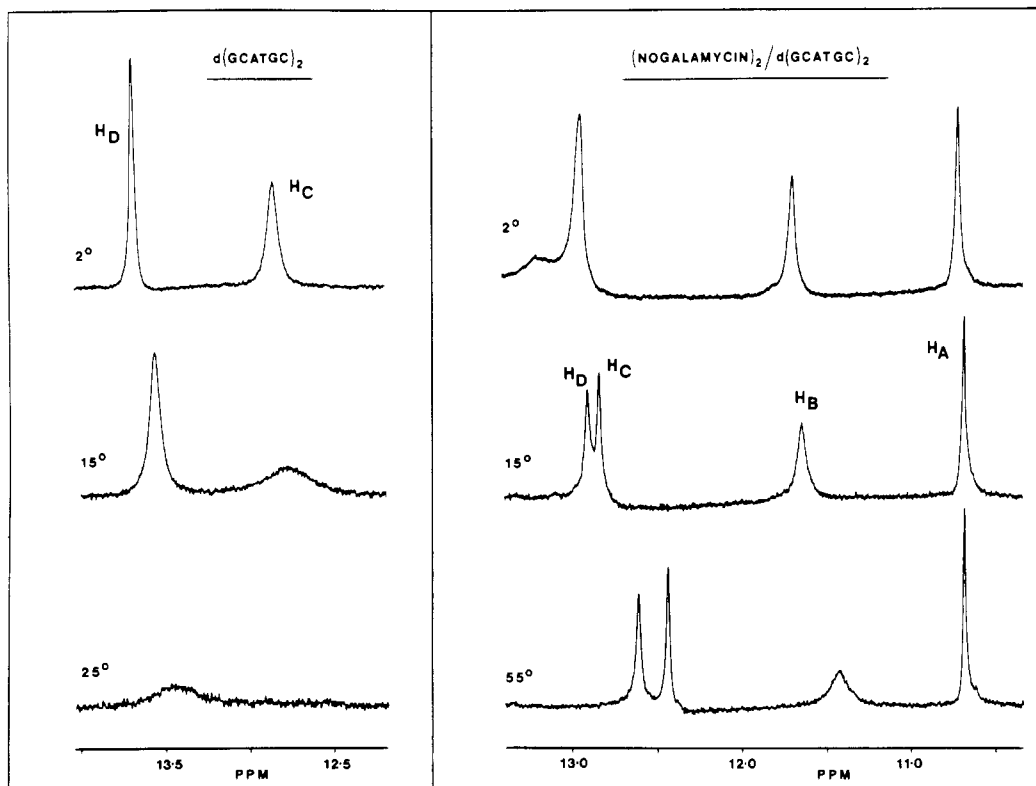
FIGURE 7: Low-field region of the ^{1}H NMR spectra of d(GCATGC)$_2$ and the (nogalamycin)$_2$/d(GCATGC)$_2$ complex recorded in 90% H$_2$O/10% D$_2$O at the temperatures indicated. Resonances H$_C$ and H$_D$ have been assigned to the imino protons of the nonterminal G·C and A·T base pairs, respectively. Resonances H$_A$ and H$_B$ in the spectrum of the complex have been attributed to the C6 and C4 phenoxy protons, respectively, as described in the text.

lowest field resonances in the complex, H$_C$ and H$_D$, are characteristic of base pair imino protons and have chemical shifts within 0.7 ppm of those of d(GCATGC)$_2$. Hence, it is proposed that resonances H$_A$ and H$_B$ are exchangeable drug protons that are shifted downfield as a result of hydrogen bonding. In the spectrum of nogalamycin in CDCl$_3$ two resonances are similarly observed at low field between 11.5 and 13.0 ppm and have been assigned to the two hydrogen-bonded phenoxy protons of the chromophore (unpublished observations). Selective irradiation of H$_D$ for 300 ms leads to the pattern of NOEs illustrated in Figure 9. This pattern is similar to that observed when irradiating the 4TN3H of the A·T base pair in the duplex alone. Intra-base-pair effects are observed to the 3AH2 and 3AN6H$_2$ which assign H$_D$ to the 4TN3H of the A·T base pair in the complex. In addition, an NOE is observed to the drug proton resonance H$_A$. Resonance H$_C$ at this stage can be tentatively assigned to the 5GN1H of the nonterminal G·C base pair. Irradiation of H$_C$ results in a large NOE on the previously assigned nonexchangeable drug resonance H$_a$. Irradiation of H$_C$ produced no effects on any protons of the A·T base pair, confirming that the integrity of the base-pair stacking is not conserved in the complex, a finding consistent with intercalation of nogalamycin between these base sets. The kinetic stabilization of the base pairs forming the drug binding site and the upfield perturbation to the chemical shifts of their imino protons that accompany drug binding are further characteristics of intercalation (Pardi et al., 1983; Feigon et al., 1984).

Other NOEs are also observed from the exchangeable drug resonances H$_A$ and H$_B$; H$_A$ gives an NOE to H$_D$ and a smaller effect to H$_C$. The broadened resonance H$_B$ gives an NOE to the drug resonance H$_A$ and smaller effects to H$_D$ and 3AH2. These effects are illustrated in Figure 9. Given a structure of the complex in which the drug chromophore is sandwiched

between the 5′-CA and 5′-TG base steps, the pattern of NOEs observed in the 1D experiments can be rationalized and the resonances H$_A$ and H$_B$ assigned to nogalamycin phenoxy protons. The proximity of H$_A$ to the imino proton of the A·T base pair and to H$_B$ leads us to suggest that H$_A$ corresponds to the hydroxyl proton on C6 and H$_B$ to the hydroxyl on C4. The configuration of the complex requires that the C6 hydroxyl be appreciably shielded from the solvent by the nogalose sugar moiety lying in the narrow groove. This notion is consistent with the extremely slow exchange rate of H$_A$ in the complex ($\Delta\nu_{1/2}$ = 5 Hz at 55 °C) and the almost invariant nature of the dependence of its chemical shift on temperature. Since H$_A$ is stacked close to the adenine ring in the complex, its observed chemical shift most likely embodies a substantial ring-current contribution. The C4 hydroxyl proton appears 0.95 ppm downfield of H$_A$ and, given the structure of the complex, would be exposed to the solvent in the major groove. This accounts for the appreciably faster exchange rate of H$_B$ ($\Delta\nu_{1/2}$ = 51 Hz at 55 °C) and the marked temperature dependence of its chemical shift.

^{31}P NMR Spectra. ^{31}P chemical shifts have been shown to be a valuable probe of the changes in backbone P–O ester bond torsional angles that accompany the intercalation of drug molecules into DNA (Patel, 1974, 1976; Gorenstein & Goldfield, 1984). Theoretical studies indicate deshielding of ^{31}P signals by up to 2 ppm for a conformational transition of the phosphodiester group from a gauche,gauche to a gauche,trans configuration (Gorenstein & Kar, 1975; Prado et al., 1979; Gorenstein, 1983, 1984). Such calculations suggest that perturbation of the C5′–O5′ torsion angle by 20–30° can result in deshielding of 0.5–1.0 ppm. To seek direct NMR evidence for changes to the helix winding accompanying intercalation of nogalamycin, we measured the ^{31}P NMR spectra of free d(GCATGC)$_2$ and the (nogalamy-
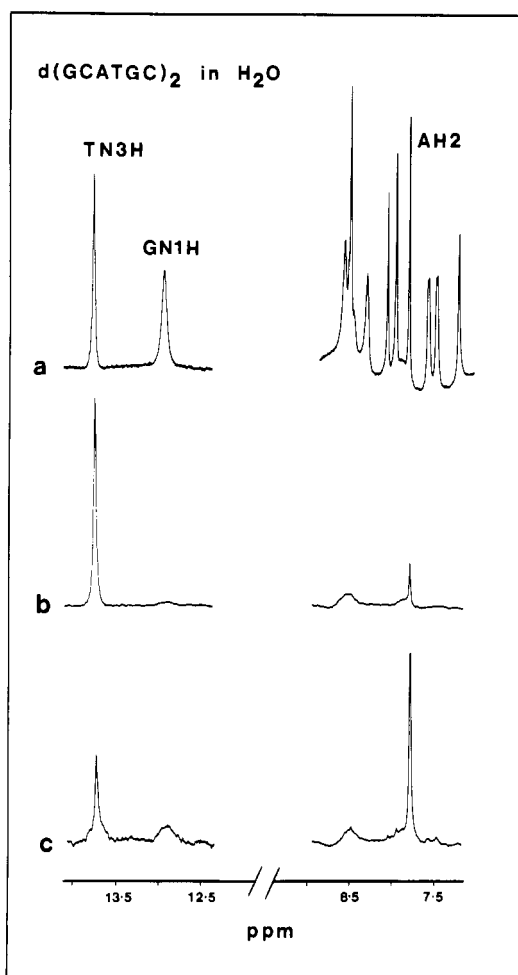
FIGURE 8: ¹H NMR spectrum and NOE difference spectra of d-(GCATGC)₂ recorded in 90% H₂O/10% D₂O at 2 °C: one-dimensional NMR spectrum of aromatic and low-field imino proton resonances (a); NOE difference spectra after 300-ms irradiation of H_D (b) and 3AH2 (c). Spectra required 512 transients with a relaxation delay of 2 s.

FIGURE 9: ¹H NMR spectrum and NOE difference spectra of the (nogalamycin)₂/d(GCATGC)₂ complex recorded at 25 °C in 90% H₂O/10% D₂O: one-dimensional NMR spectrum of aromatic and low-field exchangeable proton resonances (a); NOE difference spectra after 300-ms irradiation of H_D (b), H_C (c), H_B (d), and H_A (e). Spectra required 1024 transients with a relaxation delay of 2 s.

cin)₂/d(GCATGC)₂ complex (Figure 10). The five phosphodiester resonances of the free duplex cluster together over a small chemical shift range at −2.9 to −3.4 ppm, but in the spectrum of the complex two peaks are shifted significantly downfield from the main envelope and resonate at −2.5 and −1.6 ppm (Figure 10). Thus, in the presence of nogalamycin we do indeed find two phosphate groups whose chemical shifts are perturbed by the degree expected, given that nogalamycin is reported to have a helix unwinding angle of 18° measured by using random-sequence DNA (Gale et al., 1981).

Conclusions and Comparison with Other Work. The 28 intermolecular NOE contacts between nogalamycin and hexanucleotide permit a well-defined description of the three-dimensional structure of the complex. The dyad symmetry of the hexanucleotide, the sequence specificity of the antibiotic, and the stoichiometry of binding combine to reduce the complexity of the system to a study of the interaction of nogalamycin with the trinucleotide duplex d(GCA)·d(TGC). This is, of course, symmetrically equivalent to the complex with d(TGC)·d(GCA), and details of the interaction may be discussed in terms of either sequence. In the interests of clarity, the following discussion and summary of our findings is described with respect to a nogalamycin/d(GCA)·d(TGC) complex. Nogalamycin intercalates at the 5′-CA step with the major axis of the anthracycline chromophore aligned approximately at right angles to the major axes of the base pairs. The nogalose sugar moiety resides in the narrow groove of the
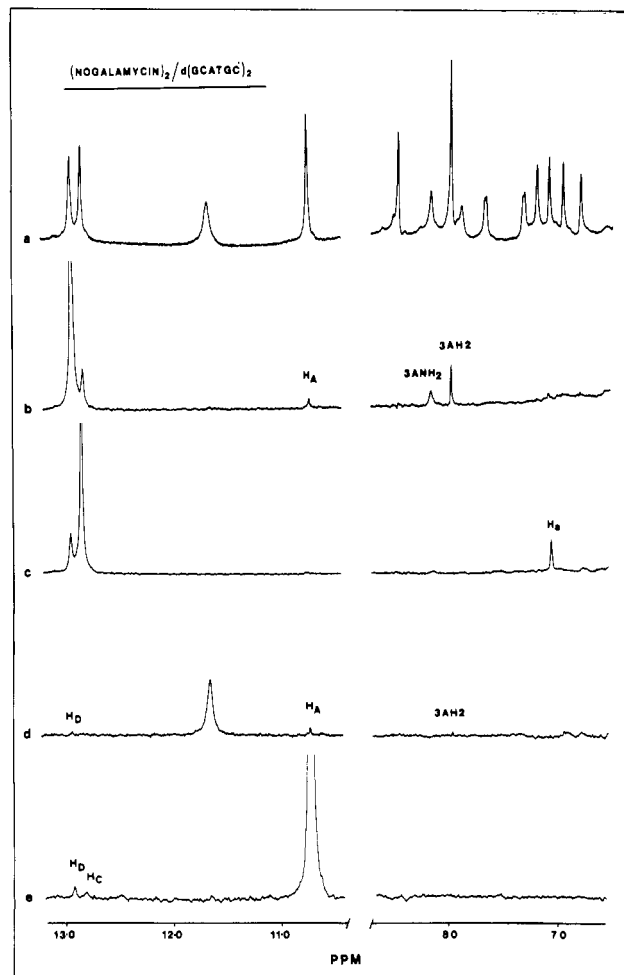
helix, and the charged bicyclic group lies in the major groove. The antibiotic is not symmetrically disposed in the intercalation cavity but is in close contact in both grooves with atoms comprising the 5′-TGC strand. The nogalose sugar stretches over all three base pairs, there being many contacts between it, the reduced anthracycline ring, the carbomethoxy group at position 10, and the deoxyribose sugars of the 5′-TGC bases. Two particularly strong contacts stand out which define the geometrical limits of the interaction, these being, at one end, that between the methyl group Me$_k$ of nogalose and the H1′ of the terminal cytosine and, at the other end, that between the carbomethoxy methyl group Me$_c$ and the H1′ of the thymine. The only intermolecular NOE contacts with the 5′-GCA strand in the narrow groove are between the nogalose methoxy group OMe$_j$ and the deoxyribose H1′ protons of adenine and cytosine, and between the nogalose anomeric proton H$_h$ and the adenine H1′. In the wide groove, intermolecular NOEs are confined to strong contacts involving the 5-methyl group of the thymine and the H$_w$ and methyl Me$_r$ protons of the nogalamycin bicyclic ring A. Corey–Pauling–Koltun (CPK) molecular models show that this necessarily places the hydroxyl and charged dimethylamino functions of the bicyclic ring in close proximity to the O6 and N7 atoms of the central guanine base and the O6 carbonyl oxygen of the terminal guanine, respectively. Thus, as found in the narrow groove, in the wide groove the antibiotic interacts predominantly with components of the 5′-TGC strand. Ob-
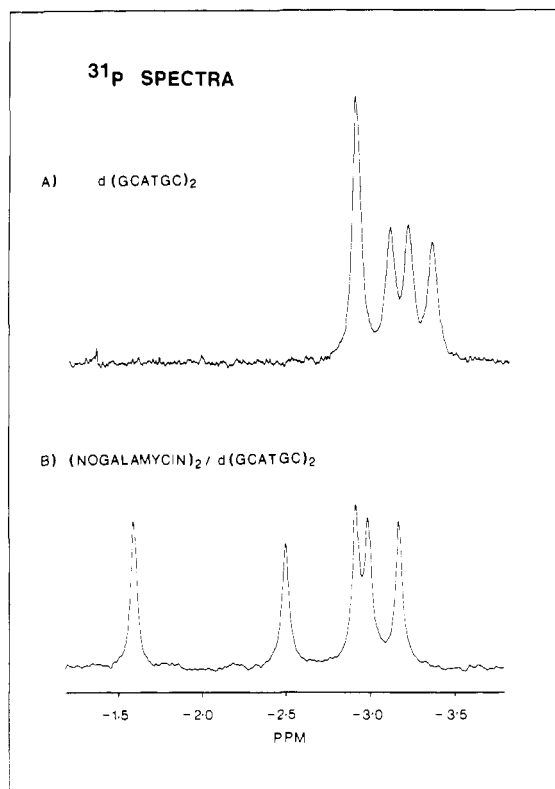
^{31}P SPECTRA

A)   d(GCATGC)$_2$

B)   (NOGALAMYCIN)$_2$ / d(GCATGC)$_2$

-1.5   -2.0   -2.5   -3.0   -3.5
PPM

FIGURE 10: ^{31}P NMR spectra of d(GCATGC)$_2$ and the (nogala-mycin)$_2$/d(GCATGC)$_2$ complex. Spectra were acquired at 20 °C, 256 transients being collected in each case. Chemical shifts are referenced to the ^{31}P resonance from the 10 mM phosphate buffer at pH 7.0.

servations of the exchangeable protons confirm that all base-pair hydrogen-bonding interactions are maintained in the complex, and there is no evidence for Hoogsteen pairing.

With the exception of those of the internal guanine, the nucleotide sugar ring puckers and glycosidic bond angles in the complex are but little perturbed from the C2'-endo, anti configuration found for the ligand-free duplex. There are, however, clear changes in these parameters for the middle guanine. The fact that these modifications do not extend to the conformation of its hydrogen-bonded cytosine and the fact that the internucleotide NOE correlations are contiguous at the 5'-CA step but are interrupted by the anthracycline ring at the 5'-TG step add further weight to the notion that the antibiotic binds primarily to the 5'-TGC strand. In addition, these findings strongly suggest that the intercalation cavity is in fact wedge-shaped, the major axes of the base pairs forming the site being tilted with respect to one another. Ring-current effects of the intercalated nogalamycin chromophore cause substantial downfield movement in chemical shift values of the deoxyribose H1', H2', and H2" protons of the thymine and central cytosine nucleotides lining the binding site. Once again, these drug-induced perturbations are more pronounced for the nucleotide in the sequence 5'-TGC. Large anthracycline-induced upfield shifts of the central guanine H8 proton, the thymine methyl group, and the imino proton of the A·T but not the G·C base pair yet again point to preferential stacking of the chromophore on the bases of the 5'-TGC strand. The selective large shift in the ^{31}P resonance frequency of two of the five phosphate groups in the hexanucleotide complex suggests that nogalamycin-induced unwinding of the helix is largely confined to the intercalation site itself. That the two downfield-shifted ^{31}P resonances are not coincident is consistent with the asymmetrical nature of the modifications

to the geometry of the nucleotides forming the cavity, and it is tempting to identify the resonance found at lowest field with the 5'-TpG phosphate and the one at next lowest field with the 5'-CpA group. Further speculation on direct measurements of the effect of nogalamycin binding on helix winding must await full assignment of the ^{31}P NMR spectrum of the complex.

The structure of the complex outlined above sheds new light on the origins of nogalamycin sequence selectivity. The principal determinants of specificity appear to be hydrogen-bonding and electrostatic interaction between the O6 and N7 atoms of the central guanine, the O6 carboxyl oxygen of the terminal guanine, and the hydroxyl and protonated dimethylamino groups of the nogalamycin bicyclic ring A. In addition, there is the potential for van der Waals interactions between the thymine methyl group and the bridging atoms (Me$_r$–O–H$_w$) of the bicyclic ring. The hydroxyl group attached to the C2' atom of ring A is well positioned for hydrogen bonding to the central guanine N7 nitrogen while, simultaneously, the nogalamycin C4' hydroxyl can bind to the O6 carbonyl oxygen. This configuration places the positively charged dimethylamino group adjacent to the O6 atom of the terminal guanine on the opposite strand, precisely in a region of highly negative electrostatic potential (Dean & Wakelin, 1980). Thus here there is the opportunity for both hydrogen-bonding and electrostatic stabilization of the complex. That such intimate involvement of a guanine N7 is likely in nogalamycin/DNA complexes finds support in the capacity of the antibiotic to inhibit N7 alkylation by dimethyl sulfate (Fox & Howarth, 1985). We are uncertain as to whether there are any interactions in the narrow groove that contribute to sequence-specific binding. Although there is the possibility for hydrogen bonding between the nogalamycin hydroxyl at position 9 and the adenine N3 nitrogen, most of the nogalamycin–DNA contacts in this groove seem to be confined to van der Waals interactions, largely between the sugar rings of the 5'-TGC strand and the hydrophobic portions of the antibiotic. The thermodynamic importance of these interactions should not be underestimated, however, as shown by the substantial loss in DNA affinity of the nogalamycin derivative lacking the nogalose moiety (Plumbridge & Brown, 1979).

We may also compare our conclusions concerning the structure of the nogalamycin–DNA complex with the predictions made by Arora (1983) and by Collier et al. (1984). While Arora (1983) correctly assigned the groove disposition of the amino and nogalose sugars, he modeled the interaction with the trinucleotide 5'-TAA and we are thus unable to comment on his proposed hydrogen-bonding scheme. Collier et al. (1984) performed molecular mechanics calculations on a nogalamycin/d(TA)$_2$ dinucleotide complex and concluded that the nogalose sugar could lie in either groove, there being two alternative sets of specific hydrogen-bonding contacts with the adenine base on the 3' side of the intercalation site. The authors generalized their results to predict that when intercalated at a 5'-CA site, the nogalose sugar would lie in the wide groove, with hydrogen-bonding contacts between the amino group of adenine and the nogalamycin carbomethoxy group. Evidently, the prediction is at odds with our findings.

Finally, to conclude, we are currently undertaking distance geometry and molecular mechanics calculations in order to refine the three-dimensional structure of the nogalamycin/hexanucleotide complex. We have recently completed, and shall report elsewhere, NMR and stopped-flow studies of the dynamics of the interaction between nogalamycin and d-(GCATGC)$_2$ that provide insights into the mechanisms

whereby the bulky sugars of nogalamycin thread through the DNA helix.

REFERENCES

Arora, S. K. (1983) *J. Am. Chem. Soc. 105*, 1328–1332.

Bhuyan, B. K., & Dietz, A. (1965) *Antimicrob. Agents Chemother. (1961-70) 1965*, 836–844.

Bhuyan, B. K., & Smith, C. G. (1965) *Proc. Natl. Acad. Sci. U.S.A. 54*, 566–572.

Bhuyan, B. K., & Reusser, F. (1970) *Cancer Res. 30*, 984–989.

Bhuyan, B. K., Blowers, C. L., & Shugars, K. D. (1980) *Cancer Res. 40*, 3437–3442.

Chazin, W. J., Wurthrich, K., Rance, M., Hyberts, S., Denny, W. A., & Leupin, W. (1986) *J. Mol. Biol. 190*, 439–453.

Chowdhury, K., Chowdhury, I., Biswas, N., & Neogy, R. K. (1978) *Indian J. Biochem. Biophys. 15*, 373–376.

Clore, G. M., & Gronenborn, A. M. (1985) *EMBO J. 4*, 829–835.

Clore, G. M., Kimber, B. J., & Gronenborn, A. M. (1983) *J. Magn. Reson. 54*, 170–173.

Collier, D. A., Neidle, S., & Brown, J. R. (1984) *Biochem. Pharmacol. 33*, 2877–2880.

Das, G. C., Dasgupta, S., & Das Gupta, N. N. (1974) *Biochim. Biophys. Acta 353*, 274–282.

Dean, P. M., & Wakelin, L. P. G. (1980) *Proc. R. Soc. London, B 209*, 453–471.

Denny, W. A., Leupin, W., & Kearns, D. R. (1982) *Helv. Chim. Acta 65*, 2372–2393.

Ennis, H. L. (1981) *Antimicrob. Agents Chemother. 19*, 657–665.

Feigon, J., Denny, W. A., Leupin, W., & Kearns, D. R. (1984) *J. Med. Chem. 27*, 450–465.

Fok, J., & Waring, M. J. (1972) *Mol. Pharmacol. 8*, 65–74.

Fox, K. R., & Waring, M. J. (1984) *Biochim. Biophys. Acta 802*, 162–168.

Fox, K. R., & Howarth, N. R. (1985) *Nucleic Acids Res. 13*, 8695–8714.

Fox, K. R., & Waring, M. J. (1986) *Biochemistry 25*, 4349–4356.

Fox, K. R., Brasset, C., & Waring, M. J. (1985) *Biochim. Biophys. Acta 840*, 383–392.

Frey, M. H., Leupin, W., Sorensen, O. W., Denny, W. A., Ernst, R. R., & Wuthrich, K. (1985) *Biopolymers 24*, 2371–2380.

Gale, E. F., Cundliffe, E., Reynolds, P. E., Richmond, M. H., & Waring, M. J. (1981) *The Molecular Basis of Antibiotic Action*, 2nd ed., pp 258–401, Wiley, London.

Gorenstein, D. G. (1983) *Prog. Nucl. Magn. Reson. Spectrosc. 16*, 1–98.

Gorenstein, D. G. (1984) in ³¹*P NMR: Principles and Applications* (Gorenstein, D. G., Ed.) Chapter 1, Academic Press, New York.

Gorenstein, D. G., & Kar D. (1975) *Biochem. Biophys. Res. Commun. 65*, 1073–1080.

Gorenstein, D. G., & Goldfield, E. M. (1984) in ³¹*P NMR: Principles and Applications* (Gorenstein, D. G., Ed.) Chapter 9, Academic Press, New York.

Gorenstein, D. G., Lai, K., & Shah, D. O. (1984) *Biochemistry 23*, 6717–6723.

Hare, D. R., Wemmer, D. E., Chou, S.-H., Drobny, G., & Reid, B. R. (1983) *J. Mol. Biol. 171*, 319–336.

Hore, P. J. (1983) *J. Magn. Reson. 55*, 283–300.

Keeler, J., & Neuhaus, J. (1985) *J. Magn. Reson. 63*, 454–472.

Kersten, W., Kersten, H., & Szybalski, W. (1966) *Biochemistry 5*, 236–244.

Krueger, W. C. (1979) *Cancer Res. 39*, 4816–4822.

Li, L. H., Kuentzel, S. L., Murch, L. I., Pschigoda, L. M., & Krueger, W. C. (1979) *Cancer Res. 39*, 4816–4818.

Muller, L., & Ernst, R. R. (1979) *Mol. Phys. 38*, 963–992.

Nilges, M., Clore, G. M., Gronenborn, A. M., Brunger, A. T., Karplus, M., & Nilsson, L. (1987) *Biochemistry 26*, 3718–3733.

Pardi, A., Morden, K. M., Patel, D. J., & Tinoco, I., Jr. (1983) *Biochemistry 22*, 1107–1113.

Patel, D. J. (1974) *Biochemistry 13*, 2396–2402.

Patel, D. J. (1976) *Biopolymers 15*, 533–558.

Plumbridge, T. W., & Brown, J. R. (1979) *Biochem. Pharmacol. 28*, 3231–3234.

Prado, F. R., Giessner-Prettre, C., Pullman, B., & Dandey, J.-P. (1979) *J. Am. Chem. Soc. 101*, 1737–1742.

Quigley, G. J., Wang, A. H.-J., Ughetto, G., van der Marel, G., van Boom, J. H., & Rich, A. (1980) *Proc. Natl. Acad. Sci. U.S.A. 77*, 7204–7208.

Reinhardt, G. G., & Krugh, T. R. (1977) *Biochemistry 16*, 2890–2895.

Scheek, R. M., Russo, N., Boelens, R., Kaptein, R., & van Boom, H. (1983) *J. Am. Chem. Soc. 105*, 2914–2916.

Sinha, R. K., Talapatra, P., Mitra, A., & Mazumder, S. (1977) *Biochim. Biophys. Acta 474*, 199–209.

States, D. J., Haberkorn, R. A., & Ruben, D. J. (1982) *J. Magn. Reson. 48*, 286–292.

Williamson, M. P. (1983) *J. Magn. Reson. 55*, 471–474.